Supplement materials to:

Seasonal variation and origins of volatile organic compounds observed during two years at a western Mediterranean remote background site (Ersa, Cape Corsica)

Cécile Debevec[1], Stéphane Sauvage[1], Valérie Gros[2], Thérèse Salameh[1], Jean Sciare[2,3], François Dulac[2], Nadine Locoge[1].

[1]IMT Lille Douai, Univ. Lille, SAGE - Département Sciences de l'Atmosphère et Génie de l'Environnement, 59000 Lille, France
[2] Equipe CAE, Laboratoire des Sciences du Climat et de l'Environnement (LSCE), Unité Mixte CEA-CNRS-UVSQ, Gif sur Yvette, 91190, France
[3] Climate and Atmosphere Research Centre, the Cyprus Institute (CyI), Nicosia, 2121, Cyprus

Correspondence to: Stéphane Sauvage (stephane.sauvage@imt-lille-douai.fr) – Cecile Debevec (cecile.debevec@imt-lille-douai.fr)

Section S1: Identification and contribution of major sources of VOCs by EPA PMF 5.0 approach

To characterize VOC concentrations measured at Ersa, we apportioned VOC sources in this study using the positive matrix factorization approach (PMF; Paatero, 1997; Paatero and Tapper, 1994) applied to our VOC concentration dataset. We used the PMF version 5.0, an enhanced tool developed by the Environmental Protection Agency (EPA) and including a multilinear engine ME-2 (Paatero, 1999), and followed the guidance on the use of PMF (Norris et al., 2014).

PMF is a tool elaborated for a multivariate factor analysis and used for the identification and the characterization of the "p" independent sources of "n" species measured "m" times at a given site. Note that the PMF mathematical theory is detailed elsewhere (Paatero, 1997; Paatero and Tapper, 1994). Concisely, the PMF method is based on the decomposition of a matrix of chemically speciated sample data (of dimension n x m) into two matrices of factor profiles (n x p) and factor contributions (p x m), interpreting each factor as a different source type. Species profiles of each source identified represent the repartition of each species into each given factor, and the amount of mass contributed by each factor to each successive individual sample represents the evolution in time of the contribution from each factor to the various species. The principle can be condensed as:

$$x_{ij} = \sum_{k=1}^{p} g_{jk} \times f_{ki} + e_{ij} = c_{ij} + e_{ij} \,, \quad (1)$$

where x_{ij} is the ith species measured concentration (in µg m^{-3} here) in the jth sample, f_{ki} the ith mass fraction from kth source, g_{jk} the kth source contribution of the jth sample, e_{ij} the residual resulting of the decomposition and c_{ij} the species reconstructed concentration. The Eq. (1) can be solved iteratively by minimizing the residual sum of squares Q following Eq. (2):

$$Q = \sum_{i=1}^{n} \sum_{j=1}^{m} \left(\frac{e_{ij}}{s_{ij}}\right)^2 \,, \quad (2)$$

with s_{ij}, the extended uncertainty (in µg m^{-3}) related to the measured concentration of the ith species in the jth sample. A user-provided uncertainty following the procedure presented in Polissar et al. (1998) is also required by the PMF tool to weight individual points. Moreover, negative source contributions are not allowed.

In order to have sufficient completeness (in terms of observation number), only VOC measurements from bi-weekly ambient air samples collected into steel canisters from 04 June 2012 to 27 June 2014 were retained in this factorial analysis. The chemical dataset includes 14 selected single or grouped VOCs, i.e. those showing significant concentration levels during the study period (see Sect. 3.3). They were divided into five compound families: alkanes (ethane, propane, i-butane, n-butane, i-pentane, n-pentane and n-hexane), alkenes (ethylene and propene), alkyne (acetylene), diene (isoprene) and aromatics (benzene, toluene, and EX, the sum of ethylbenzene, m,p-xylenes and o-xylene). The final VOC dataset encompassed 152 atmospheric data points having a time resolution of 4 hours. Moreover, the data processing and quality analysis of the VOC dataset are presented in the supplement material of Debevec et al. (2017).

In order to optimize the PMF solution, the first step consisted in carrying out numerous successive base runs considering an incremented factor number. Results were analysed so as to identify the optimal number of factors according to

the protocol defined by Sauvage et al. (2009). Diverse statistical indicators and the physical meaning of factor profiles have also to be taken into account in the selection of the optimal solution. Generally, the non-negativity constraint alone is considered not enough to obtain a unique solution. To reduce the number of solutions, one possible approach is to rotate a given solution and assess the obtained results with the initial solution. Consequently, the second step relies on the exploration of the rotational freedom of the PMF solution selected by acting on the F_{peak} parameter (Paatero et al., 2005; Paatero et al., 2002) following recommendations of Norris et al. (2014) so as to reach an optimized final solution. As a result, a five-factor PMF solution has been chosen in this study considering a F_{peak} parameter fixed at 0.8 which allowed a finer decomposition of the VOC dataset following an acceptable change of the Q-value (Norris et al., 2014).

Section S2: Identification of potential emission areas by CF approach

In order to investigate potential emission regions contributing to long-distance pollution transport to the receptor site, source type contributions from the PMF were coupled with back-trajectories under a statistical approach. To achieve this, the concentration field (CF) statistical method established by Seibert et al (1994) was chosen in the present study.

The CF approach relies on the attribution of concentrations of a variable measured at a receptor site along respective back-trajectories arriving at this site. In a second step, the trajectory map is gridded in order for the attributed concentrations in a given cell to be weighted by the residence time that air parcels spent in the considered cell (Eq. (3); Michoud et al., 2017):

$$\log\left(\overline{C_{ij}}\right) = \frac{\sum_{L=1}^{M} \log(C_L) \times n_{ij-L}}{\sum_{L=1}^{M} n_{ij-L}} = \frac{1}{n_{ij}} \sum_{L=1}^{M} \log(C_L) \times n_{ij-L}, \quad (3)$$

with $\overline{C_{ij}}$ the attributed concentration of the ijth grid cell, C_L the concentration observed when the back-trajectory L reached the measurement site, n_{ij-L} the number of points of the back-trajectory L contained in the ijth grid cell, n_{ij} the number of points of the total number of back-trajectories contained in the ijth grid cell, and M the total number of trajectories.

Section S3: Comparisons of VOC measurements with other ones performed at Ersa

One hundred of 3-h-integrated air samples were collected at Ersa on DNPH cartridges from 29 June to 11 July 2012 at a frequency of 8 samples per day. These air samples were collected and analyzed following the same protocol as the one presented in Sect. 2.2.1. Additionally, the ChArMEx SOP-1b (special observation period 1b) field campaign took place from 15 July to 5 August 2013 at Ersa. During this intensive field campaign, more than 80 VOCs were measured by different on-line and off-line techniques which were deeply presented in Michoud et al. (2017) and summarized in Table S3-1. Furthermore, formaldehyde measurements realized during the SOP-1b field campaign with DNPH cartridges are used in this study. Finally, around 70 3-h-integrated air samples were collected at Ersa from 26 June to 10 July 2014 on DNPH cartridges (54 samples realized at a frequency of 4 cartridges per day from 6h-18h UTC) and on stainless steel canisters (20 samples realized at a frequency of 3 canisters per day from 9h-18h UTC). These air samples were collected and analyzed following the same protocol as the one presented in Sect. 2.2.1. Benefiting from all these measurements, they were confronted with the two years of VOC measurements investigated in this study, in order to examine the representativeness of the study period in terms of summer concentration levels and variations. Time series of concentrations of selected VOCs, biogenic and anthropogenic compounds and OVOCs, are depicted in Figs S3-1, S3-2 and S3-3, respectively.

Table S3-1: Technical details of the set-up for VOC measurement during the intensive field campaigns realized at Ersa in summers 2012, 2013 and 2014.

Field campaign	Instrument	Time resolution	Species observations used in this study	References
Summer 2012	**Off-line DNPH**	180 min	formaldehyde, acetaldehyde, acetone and MEK	Detournay, 2011; Detournay et al., 2013
Summer 2013 (SOP-1b)	**On-line PTR-TOF-MS**	10 min	isoprene, acetaldehyde, acetone and MEK	Michoud et al., 2017
	On-line GC-FID-FID	90 min	ethane, propane, n-butane, n-pentane, ethylene, acetylene, benzene	Michoud et al., 2017
	On-line GC-FID-MS	90 min	α-pinene, β-pinene and limonene	Michoud et al., 2017
	Off-line DNPH	180 min	formaldehyde	Detournay, 2011; Detournay et al., 2013
Summer 2014	**Off-line DNPH**	180 min	formaldehyde, acetaldehyde, acetone and MEK	Detournay, 2011; Detournay et al., 2013
	Off-line steel canisters	180 min	ethane, propane, n-butane, n-pentane, ethylene, acetylene, benzene, isoprene	Sauvage et al., 2009

During the intensive field campaign of summer 2013, biogenic compounds were measured on-line by different techniques (PTR-TOF-MS or GC-FID-MS - Table S3-1). Significant concentration levels of biogenic VOCs were measured during this summer field campaign (e.g. isoprene concentrations up to 3.5 µg.m^{-3} – Fig. S1-1). α-Pinene concentrations during the SOP-1b campaign were of the same range than summer concentrations measured off-line during the observation field campaign while isoprene concentrations were observed at higher concentrations during the SOP-1b, which can be partly related to the better time resolution and the temporal coverage of measurements. Note that isoprene daily maximal concentrations measured during the summer 2013 campaign were variable in relation to temperature variations (Kalogridis, 2014; Michoud et al., 2017). Additionally, isoprene concentrations measured during the summer 2014 field campaign were low but were in consistency with isoprene concentrations observed in June 2014.

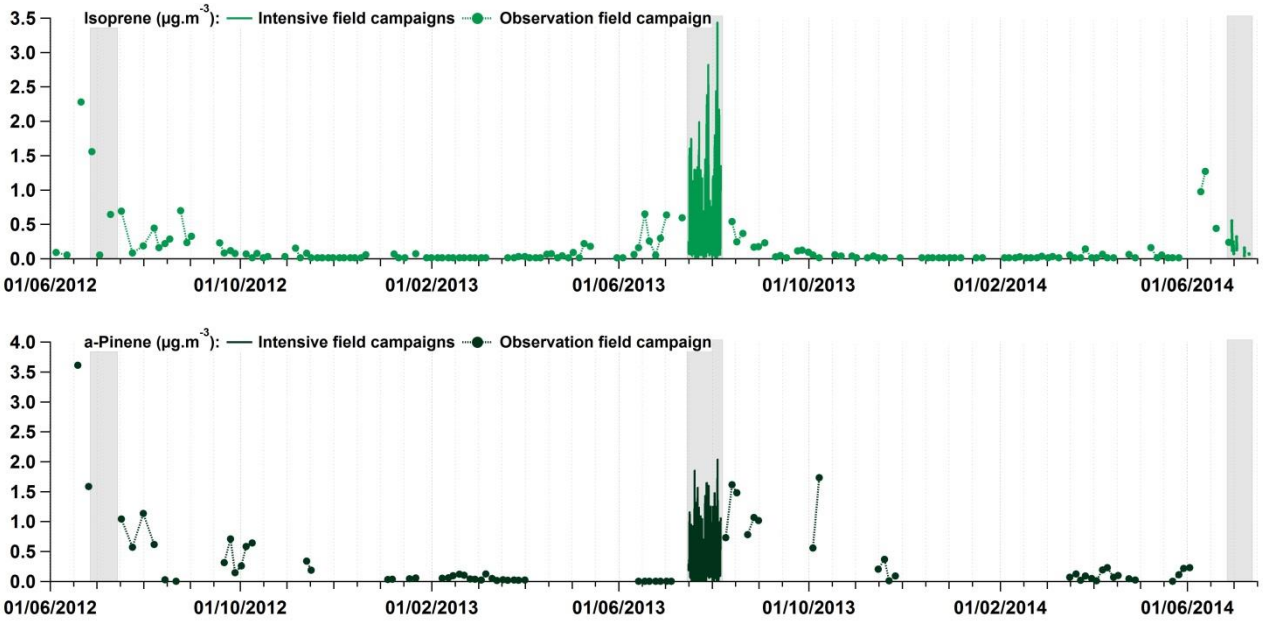

Figure S3-1: Time series of concentrations of a selection of biogenic VOCs (expressed in µg m^{-3}) measured during the different field campaigns conducted at Ersa. Grey rectangles pinpoint periods when intensive field campaign were realized. Time is given in UTC.

Anthropogenic VOC concentrations were measured with an on-line GC-FID-FID during the SOP-1b campaign and with stainless steel canister during the summer 2014 field campaign (Table S3-1). Low anthropogenic VOC concentration levels were noticed during the summer 2013 and 2014 field campaigns (Fig. S3-2) and, whatever their lifetime in the atmosphere, these concentrations were in consistency with seasonal variations described in Sect. 3.4.2. These findings can suggest that the annual temporal coverage of VOC measurements realized over the two years was sufficiently adapted to well characterize VOC concentration variations (at seasonal scale).

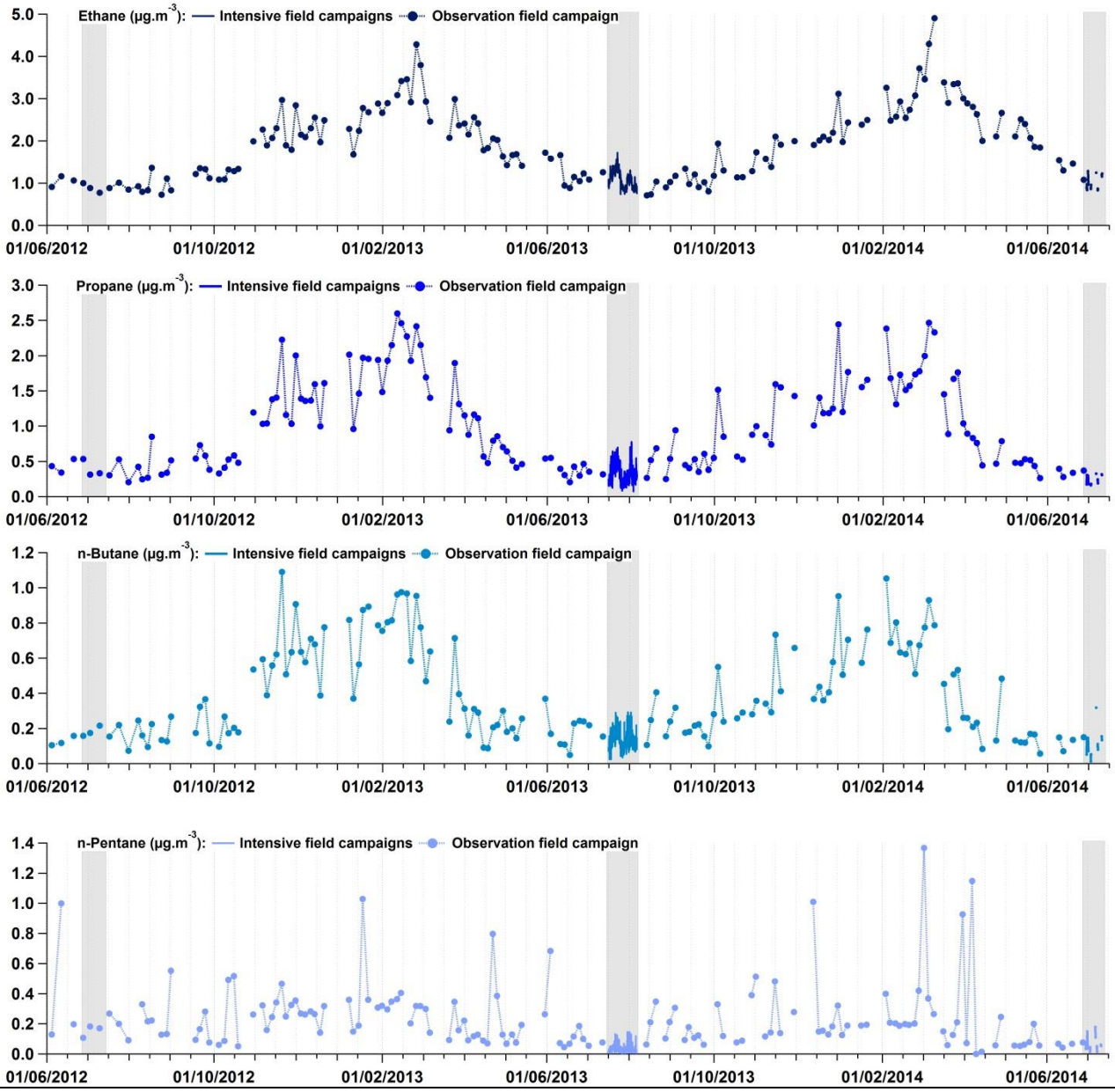
Ethane (µg.m-3): Intensive field campaigns Observation field campaign
5.0
4.0
3.0
2.0
1.0
0.0
01/06/2012
01/10/2012
01/02/2013
01/06/2013
01/10/2013
01/02/2014
01/06/2014
Propane (µg.m-3): Intensive field campaigns Observation field campaign
3.0
2.5
2.0
1.5
1.0
0.5
0.0
01/06/2012
01/10/2012
01/02/2013
01/06/2013
01/10/2013
01/02/2014
01/06/2014
n-Butane (µg.m-3): Intensive field campaigns Observation field campaign
1.2
1.0
0.8
0.6
0.4
0.2
0.0
01/06/2012
01/10/2012
01/02/2013
01/06/2013
01/10/2013
01/02/2014
01/06/2014
n-Pentane (µg.m-3): Intensive field campaigns Observation field campaign
1.4
1.2
1.0
0.8
0.6
0.4
0.2
0.0
01/06/2012
01/10/2012
01/02/2013
01/06/2013
01/10/2013
01/02/2014
01/06/2014

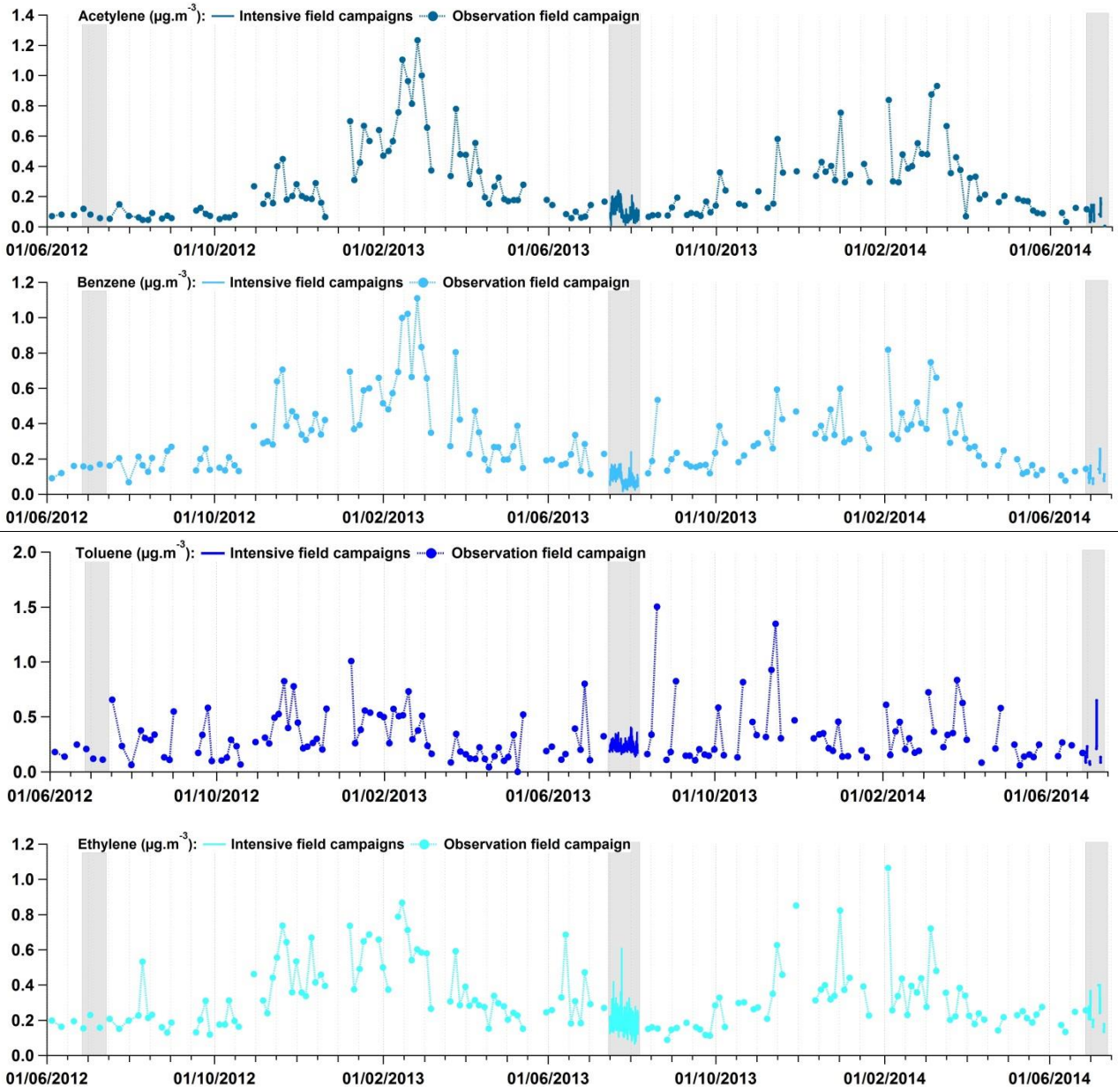

Figure S3-2: Time series of concentrations of a selection of anthropogenic VOCs (expressed in µg m^{-3}) measured during the different field campaigns conducted at Ersa. Grey rectangles pinpoint periods when intensive field campaign were realized. Time is given in UTC.

During the summer 2012 and 2014 field campaigns, OVOCs were measured off-line using DNPH cartridges. During the summer 2013 campaign, they were also measured with proton transfer reaction time-of-flight mass spectrometer (PTR-

TOF-MS - Table S3-1). OVOC concentration levels during the three summer field campaigns (Fig. S3-3) were in consistency with seasonal variations described in Sect. 3.4.3.

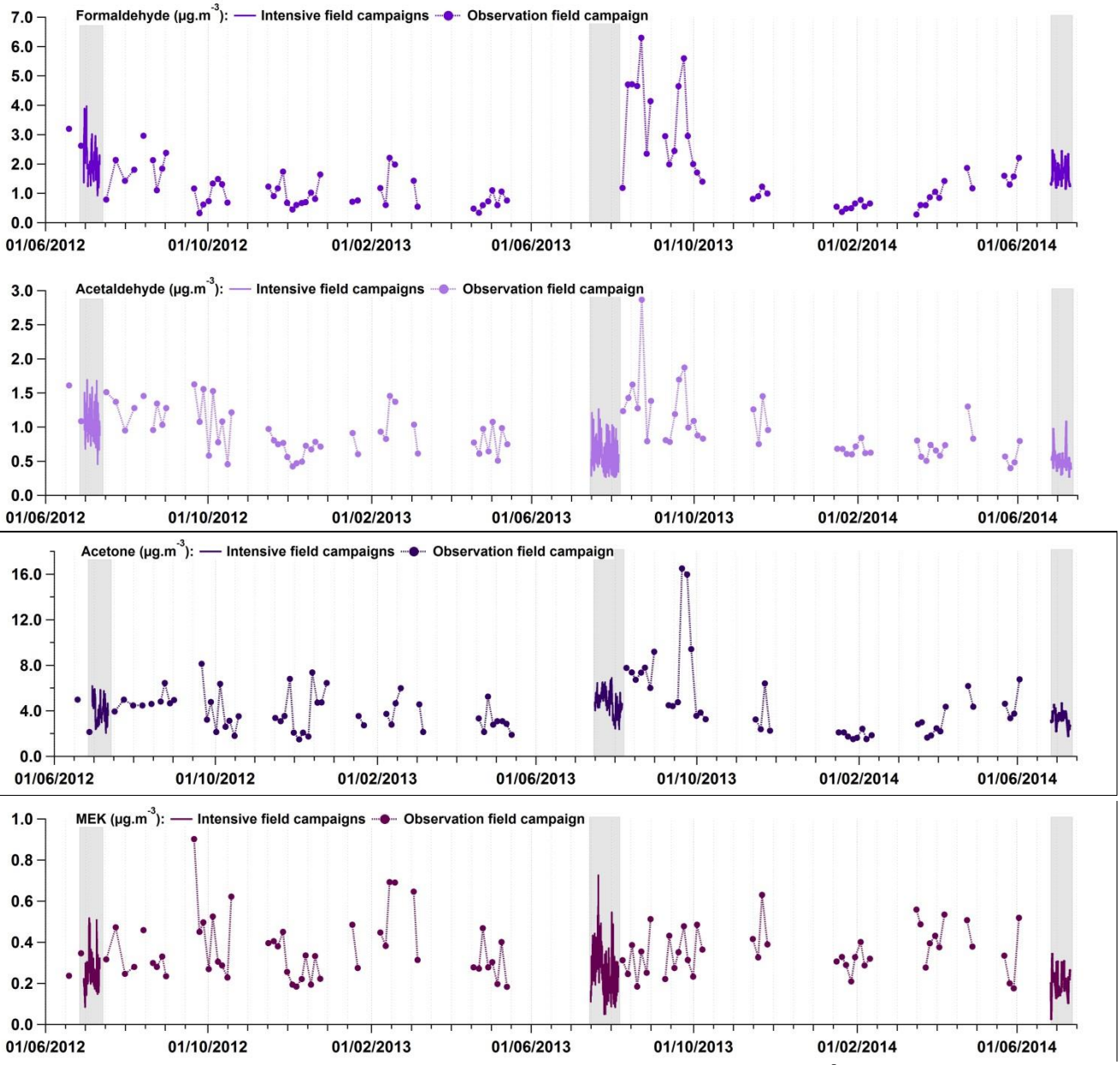

Figure S3-3: Time series of concentrations of a selection of oxygenated VOCs (expressed in µg m^{-3}) measured during the different field campaigns conducted at Ersa. Grey rectangles pinpoint periods when intensive field campaign were realized. Time is given in UTC.

Section S4: Comparisons of VOC source apportionment with previous one performed at Ersa

The 5-factor PMF solution, modelled with the two year observation field campaign VOC dataset (from June 2012 to June 2014) was compared with the PMF solution modelled with the SOP-1b VOC dataset (from 15 July to 5 August 2013 - Michoud et al., 2017), composed of 6 factors, namely primary biogenic factor, secondary biogenic factor, short-lived anthropogenic factor, medium-lived anthropogenic factor, long-lived anthropogenic factor and oxygenated factor. Note that the SOP-1b PMF source apportionment was performed on a dataset of 42 VOCs, including oxygenated compounds and collected with three different on-line techniques (see Sect. S3 and Michoud et al., 2017). Figure S4-1 compares the average relative contribution of each factor to VOC concentrations monitored during the two field campaigns.

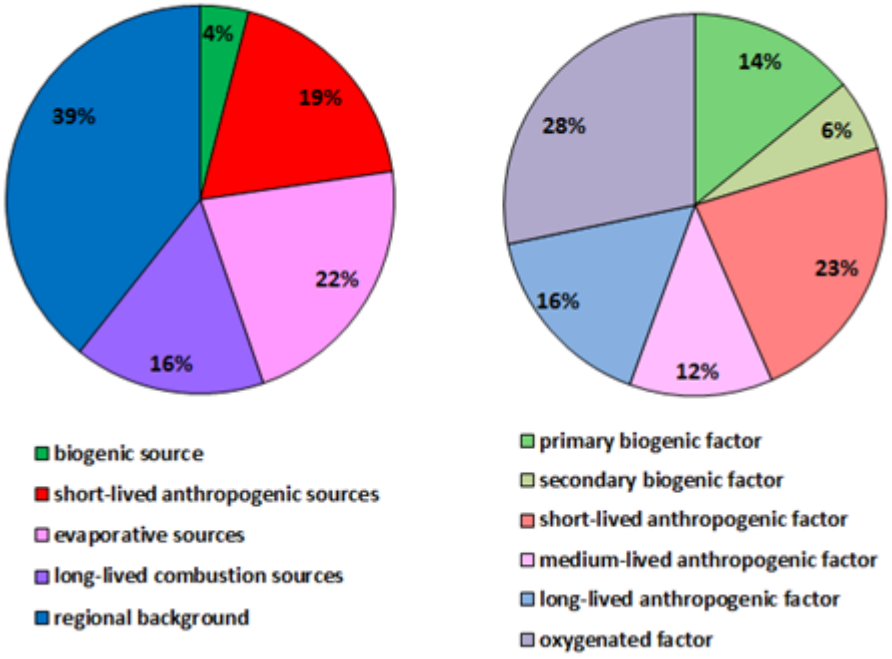

Figure S4-1: Relative factor contributions (expressed in %) to the two year VOC concentrations (on the left) compared to relative factor contributions to the SOP-1b VOC concentrations (on the right).

Firstly, the biogenic source (factor 1 – this study) was mainly composed of isoprene like the SOP-1b primary biogenic factor. The latter also explained a large portion of monoterpene concentrations along with from 11 to 15% of some OVOC concentrations (carboxylic acids, methanol and acetone). Even if monoterpenes were not integrated to the PMF analysis realized with the two years of VOC observations, considering the number of samples realized, α-pinene VOC concentration variations discussed in Sect. 3.4.1 highlighted that α-pinene showed significant concentrations in fall while isoprene concentrations were low, suggesting that an additional source could influence α-pinene concentrations observed at Ersa.

Moreover, the SOP-1b primary biogenic factor contributed of 14% to the VOC total mass measured in summer 2013, partly considering the contribution of OVOCs to this factor (~60% of the factor contribution). On the other hand, the biogenic source contribution was only of 4% to the total VOC mass measured during the two years studied but was higher in summer (12 and 15% during summers 2012 and 2013, respectively).

The observation field campaign PMF solution identified three anthropogenic factors (factors 2-4) and the regional background (factor 5) as among the main contributors to VOC concentrations impacting Ersa during two years, despite the reduced number of atmospheric data observations and the fact that primary anthropogenic VOCs were characterized by almost the same seasonal variation (Sect. 3.4.2). These factors have proved to be globally in consistency with primary anthropogenic factors identified by Michoud et al. (2017), despite the different number of VOCs considered in the two PMF analyses.

Short-lived anthropogenic sources (factor 2 – this study) explained a large portion of ethylene, propene, toluene and C_8 aromatic compounds concentrations observed at Ersa during two years similarly as the SOP-1b short-lived anthropogenic factor during summer 2013. The two factors contributed similarly to the VOC total mass (19 and 23% for observation field campaign short-lived anthropogenic sources and SOP-1b short-lived anthropogenic factor, respectively) observed at the receptor site. Note that some OVOCs contributed significantly to SOP-1b short-lived anthropogenic factor, such as formic acid, acetic acid, propionic acid and acetone (~ 61% of the factor contribution), enhancing its relative contribution to the VOC total mass. Furthermore, short-lived anthropogenic sources from the two-year VOC dataset revealed different origins according to seasons.

Evaporative sources (factor 3 – this study) and the SOP-1b medium-lived anthropogenic factor have chemical profiles marked by C_4-C_6 alkanes. Nevertheless, evaporative sources explained a higher portion of i-butane and n-butane concentrations observed at Ersa during the two years studied compared to the SOP-1b medium-lived anthropogenic factor contributions to these concentrations during summer 2013. SOP-1b medium-lived anthropogenic factor contributed of 12% to VOC concentrations during summer 2013 while evaporative source contribution was of 22% to VOC concentrations during the two years studied, partly considering their higher contribution especially in winter. Evaporative sources and SOP-1b medium-lived anthropogenic factor were of the same origins as they showed higher contributions when Ersa received French and European air masses.

SOP-1b long-lived anthropogenic factor was mainly composed of ethane, acetylene, propane and benzene and was consistent with chemical profiles characterizing long-lived combustion sources (factor 4 – this study) and regional background (factor 5 – this study). Regional background and long-lived combustion sources explained the integrality of ethane and acetylene concentrations, respectively while SOP-1b long-lived anthropogenic factor explained 58% of ethane concentrations and 44% of acetylene concentrations (Michoud et al., 2017). These findings can suggest that the PMF model, applied to the two years of VOC dataset, mostly pinpointed distant origins impacting ethane and acetylene concentrations measured at Ersa, which may be related to the temporal coverage and the time resolution of VOC measurements realized during two years. Moreover, the two year PMF solution allowed to deconvoluate long-lived combustion sources, partly attributed to residential heating and with regional origins, from the regional background and showed a higher contribution of regional background

(39% to VOC mass) than the long-lived combustion sources (16%). The high temperature in summer probably induced a limited use of heating systems that could explain why the PMF model performed with the SOP-1b VOC database did not identify separately these two distant sources and the relatively low contribution of SOP-1b long-lived anthropogenic factor to VOC mass (16%). Note that, regional background contributions were of the same range in winters 2013 and 2014 (Figs. 9 and 10) while long-lived combustion sources showed higher contributions in winter 2013 compared to winter 2014 ones, which may have participated to the deconvolution of these sources by the PMF model. The SOP-1b long-lived anthropogenic factor, long-lived combustion sources and regional background were of the same origins as they showed higher contributions especially when Ersa received European air masses.

Finally, the incorporation of OVOCs in the SOP-1b source apportionment analysis allowed to identify and characterize two secondary sources, namely secondary biogenic factor and oxygenated factor. SOP-1b secondary biogenic factor only contributed of 6% to VOC mass measured in summer 2013 and was mainly composed of methyl vinyl ketone (MVK), methacrolein (MACR), pinonaldehyde and nopinone. These compounds are specific oxidation products of primary biogenic VOCs (isoprene, α-pinene and β-pinene) which were emitted in the vicinity of the site (Michoud et al., 2017). Oxygenated factor was mainly composed of carboxylic acids (explained 54, 43 and 28% of formic acid, acetic acid and propionic acid concentrations, respectively), alcohols (e.g. 49% of methanol concentrations) and carbonyl compounds (e. g. 57, 18 and 21% of acetone, acetaldehyde and MEK concentrations, respectively). Most of these species can result from the photochemical oxidation of both anthropogenic and biogenic VOCs. Oxygenated factor was found to be the largest contributor to VOC concentrations observed at Ersa (28% of the total VOC mass). Therefore, the measured OVOCs at Ersa were approximately half oxidation products of VOCs and half primary VOCs (Michoud et al., 2017).

As a conclusion, the contribution of both experimental strategies, to characterize the main sources influencing VOC levels observed at the receptor site of pollution impacting the Western Mediterranean region, was hence investigated in this section. On one hand, the SOP-1b intensive field campaign occurred in summer and offered good conditions to monitor at a time anthropogenic sources, influenced by several geographic origins, along with biogenic local sources and secondary oxygenated sources, and to assess to their diurnal variations. On the other hand, the observation field campaign had the advantage to cover two complete years in order to monitor seasonal and interannual variations of main primary sources impacting VOC concentrations observed at the receptor site. This larger time scale of VOC measurements also helped to deconvoluate long-lived combustion sources from regional background. Nevertheless, the time resolution of VOC measurement of the 2-yr period (4 hours compared to 1 hour and a half during the SOP-1b period) and the limited number of sampling days during this study period did not help to support the clear deconvolution of the 5 factors, as factors related to anthropogenic sources were quite correlated between them (as a consequence of their seasonal variations – see Sect. 3.5; and unlike SOP-1b anthropogenic sources showing Pearson correlation factors from -0.5 to 0.1). Finally, the incorporation of OVOCs in the source apportionment had little impact on the identification of main primary sources influencing VOC concentrations observed at the receptor site but can modify their relative contributions, emphasizing the contribution of local biogenic/anthropogenic sources and decreasing the contribution of regional anthropogenic sources.

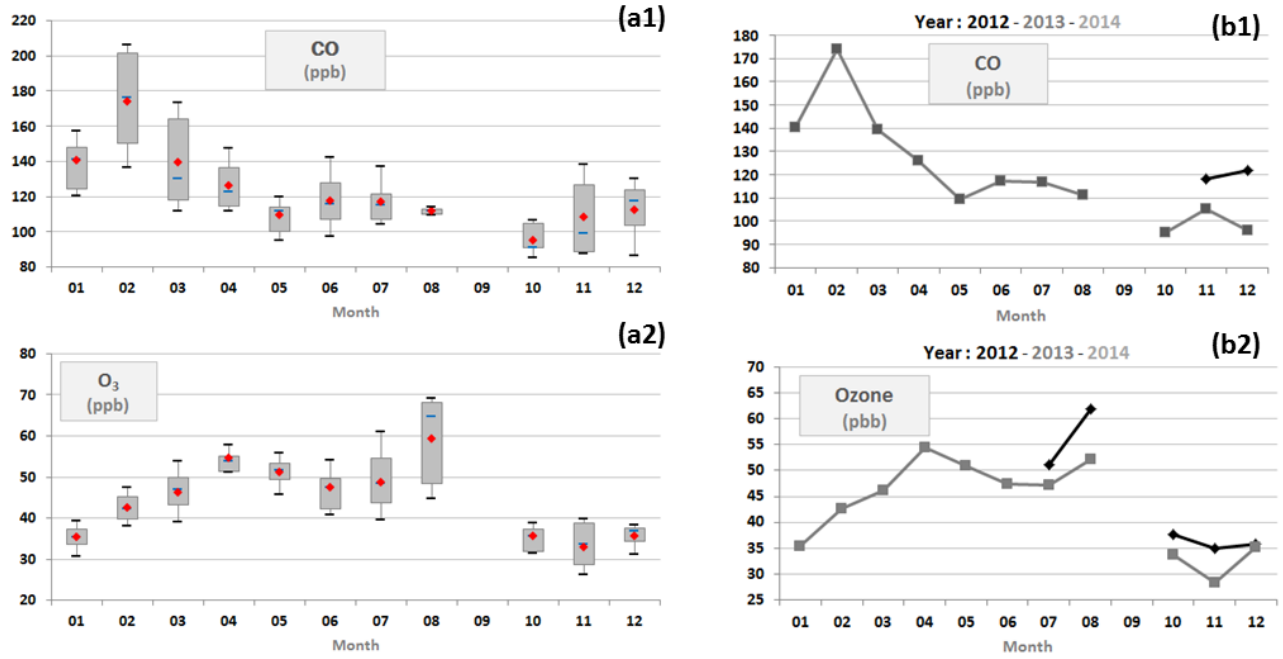

Figure S1: (a) Monthly variations in gas concentrations (CO and O_3 expressed in ppb) represented by box plots and (b) their average values as a function of the year. Blue solid line represents the median value, the red marker represents the mean value and the box shows the interquartile range. The bottom and the top of box depict the first and the third quartiles (i.e. Q1 and Q3). The ends of the whiskers correspond to first and the ninth deciles (i.e. D1 and D9). Note that, gas data used in this study were restricted to periods when VOC measurements were realized.

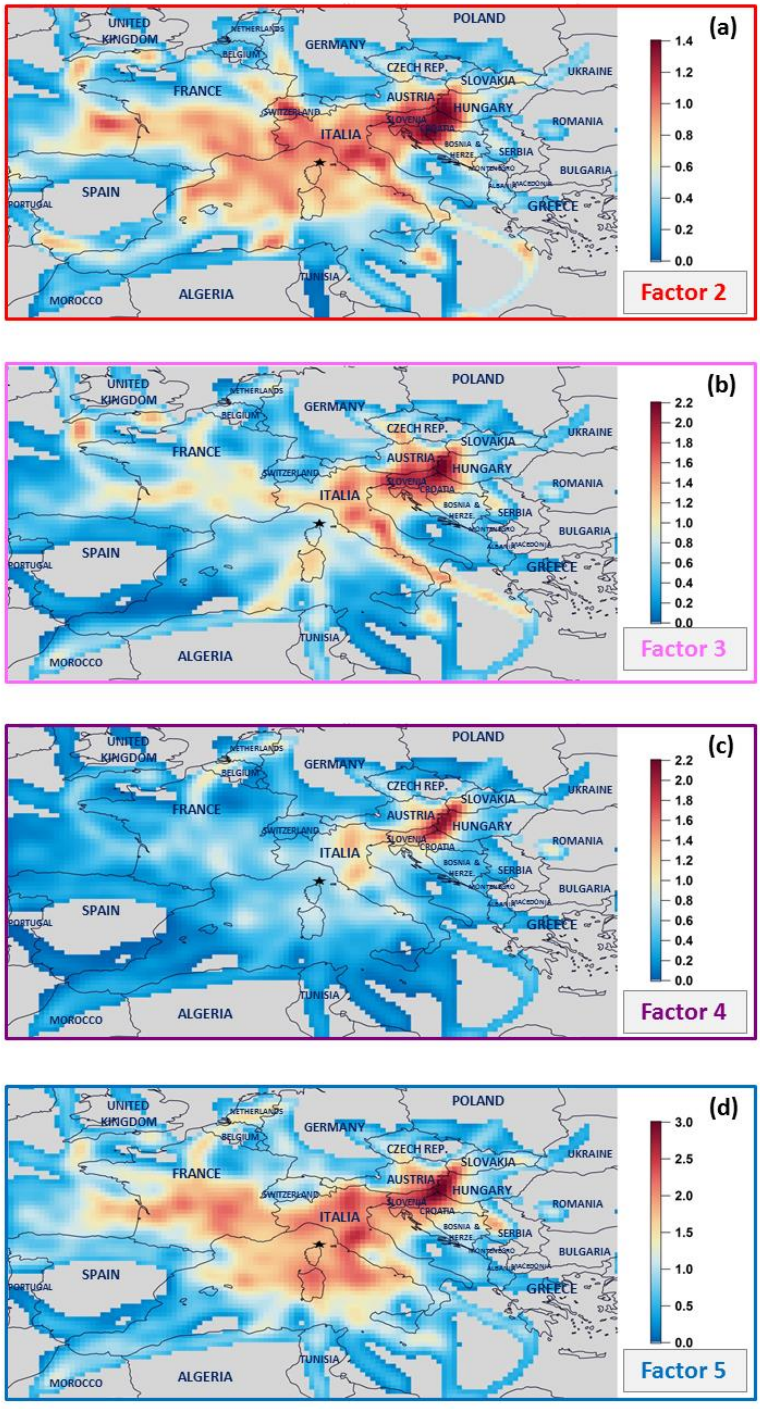

Figure S2: Potential source area contributions to factors 2-5 using the CF model. Contributions are expressed in µg m^{-3}. VOC factors: factor 2 - short-lived anthropogenic sources; factor 3 – evaporative sources; factor 4 – long-lived combustion sources; factor 5 – regional background.

Temperature anomalies (in °C)

Winter 2013

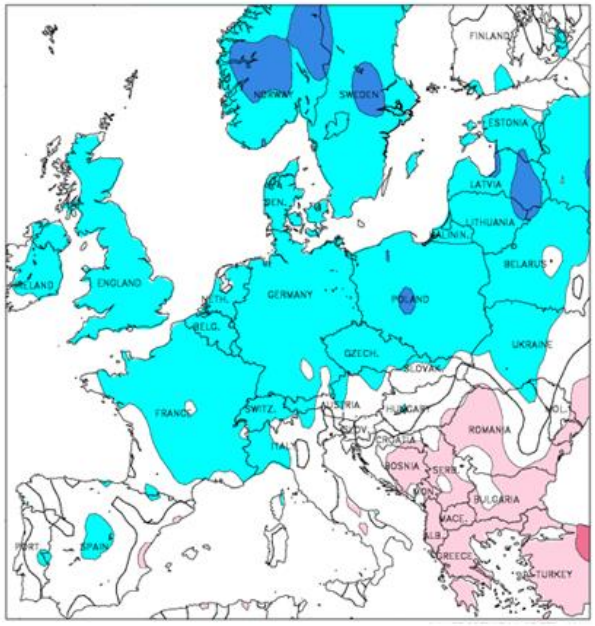

January 2014

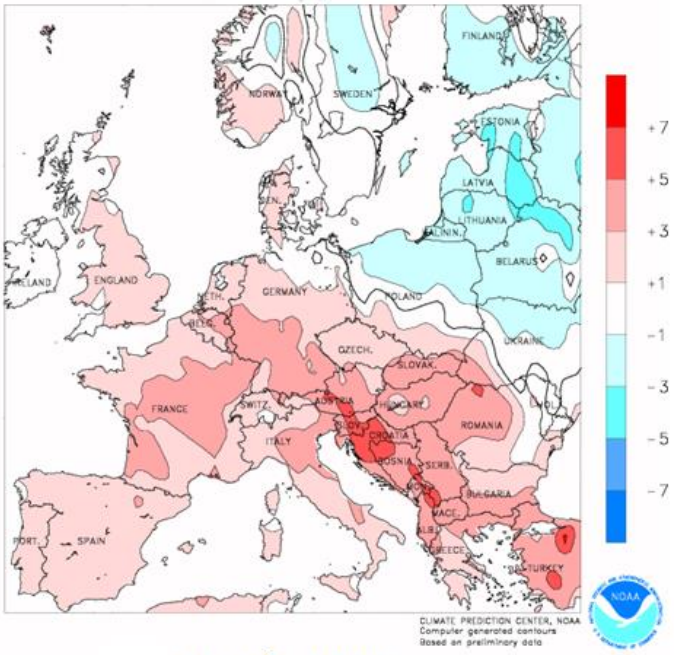

February 2014

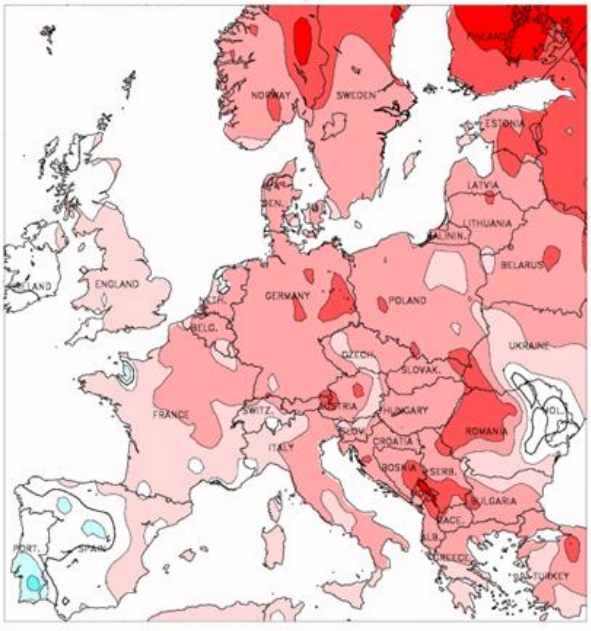

March 2014

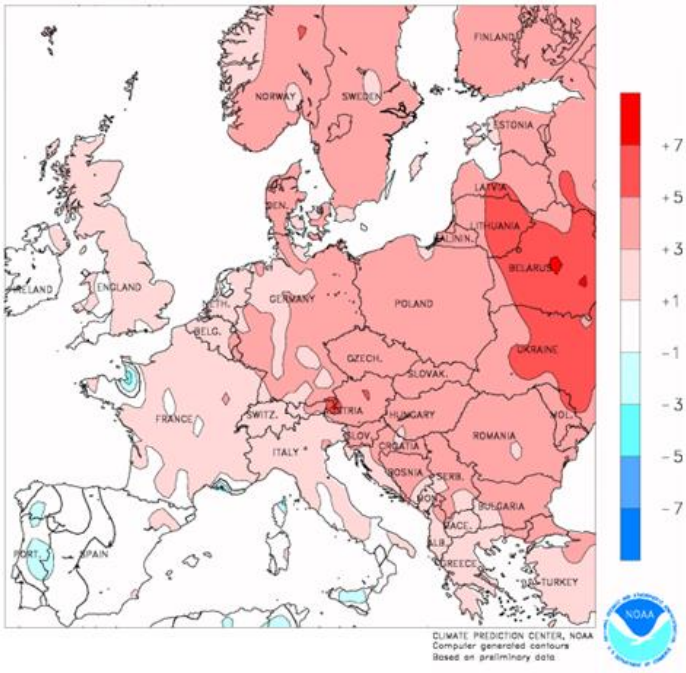

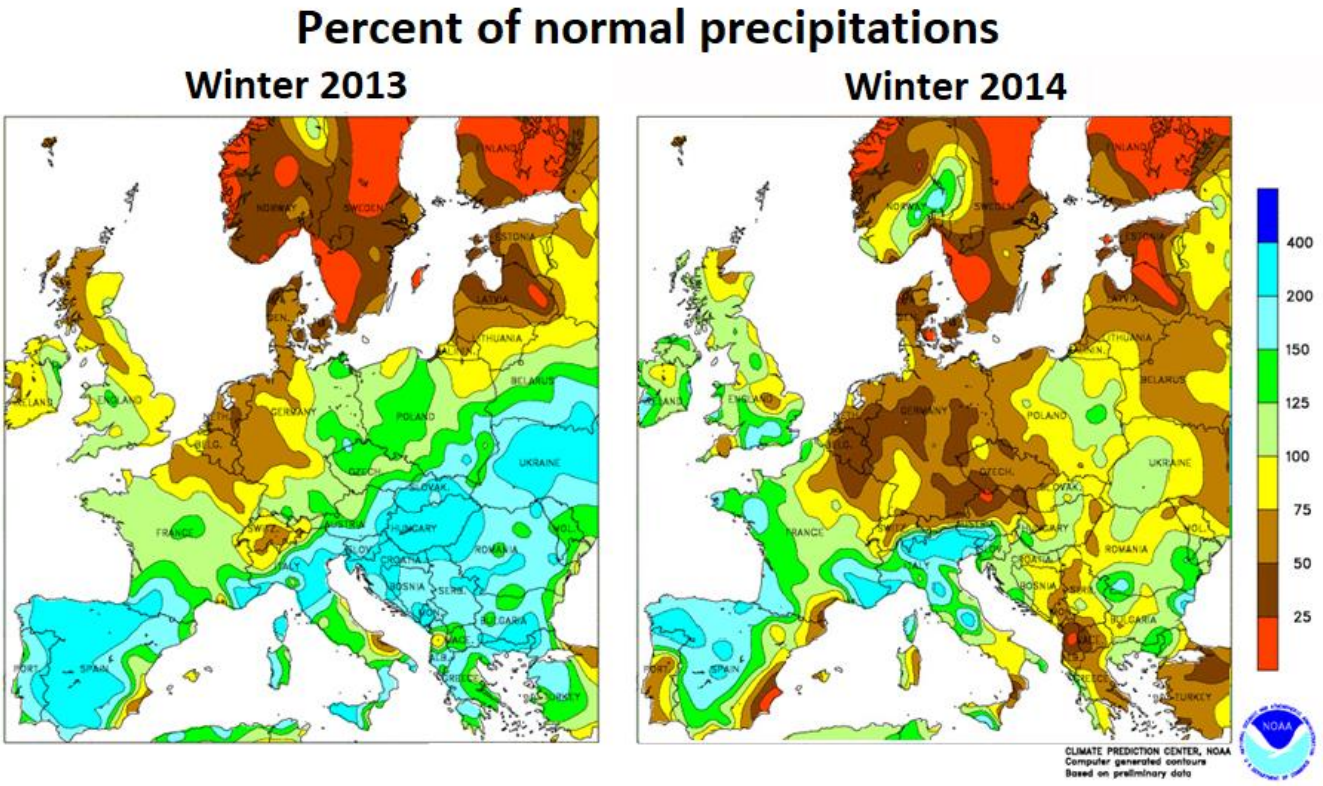

Figure S3: Temperature anomalies and percent of normal precipitations in winters 2013 and 2014 in Continental Europe. Simulation realized by the Climate prediction center of the National Oceanic and Atmospheric Administration (https://www.cpc.ncep.noaa.gov/products/analysis_monitoring/regional_monitoring/europe.html, last access: 03/04/2020). Normal values are calculated using the average of monthly (or quarterly) values for 1981-2010 period.

References

Debevec, C., Sauvage, S., Gros, V., Sciare, J., Pikridas, M., Stavroulas, I., Salameh, T., Leonardis, T., Gaudion, V., Depelchin, L., Fronval, I., Sarda-Esteve, R., Baisnée, D., Bonsang, B., Savvides, C., Vrekoussis, M., and Locoge, N.: Origin, and variability in volatile organic compounds observed at an Eastern Mediterranean background site (Cyprus), Atmos. Chem. Phys., 17, 11355–11388, doi:10.5194/acp-17-11355-2017, 2017.

Detournay, A., Sauvage, S., Locoge, N., Gaudion, V., Leonardis, T., Fronval, I., Kaluzny, P., and Galloo, J. C.: Development of a sampling method for the simultaneous monitoring of straight-chain alkanes, straight-chain saturated carbonyl compounds, and monoterpenes in remote areas, J. Environ. Monit., 13, 983–990, doi:10.1039/c0em00354a, 2011.

Detournay, A., Sauvage, S., Riffault, V., Wroblewski, A., and Locoge, N.: Source, and behavior of isoprenoid compounds at a southern France remote site, Atmos. Environ., 77, 272–282, doi:10.1016/j.atmosenv.2013.03.041, 2013.

Kalogridis, A.: Caractérisation des composés organiques volatils en région méditerranéenne, Université Paris Sud - Paris XI. [online] Available from: https://tel.archives-ouvertes.fr/tel-01165005, 2014.

Michoud, V., Sciare, J., Sauvage, S., Dusanter, S., Léonardis, T., Gros, V., Kalogridis, C., Zannoni, N., Féron, A., Petit, J. E., Crenn, V., Baisnée, D., Sarda-Estève, R., Bonnaire, N., Marchand, N., Dewitt, H. L., Pey, J., Colomb, A., Gheusi, F., Szidat, S., Stavroulas, I., Borbon, A., and Locoge, N.: Organic carbon at a remote site of the western Mediterranean Basin: Sources, and chemistry during the ChArMEx SOP2 field experiment, Atmos. Chem. Phys., 17, 8837–8865, doi:10.5194/acp-17-8837-2017, 2017.

Norris, G., Duvall, R., Brown, S., and Bai, S.: EPA Positive Matrix Factorization (PMF) 5.0 Fundamentals, and User Guide Prepared for the US Environmental Protection Agency Office of Research, and Development, Washington, DC. [online] Available from: https://www.epa.gov/sites/production/files/2015-02/documents/pmf_5.0_user_guide.pdf, 2014.

Paatero, P.: Least squares formulation of robust non-negative factor analysis, Chemom. Intell. Lab. Syst., 37, 23–35, doi:10.1016/S0169-7439(96)00044-5, 1997.

Paatero, P.: The Multilinear Engine—A Table-Driven, Least Squares Program for Solving Multilinear Problems, Including the n-Way Parallel Factor Analysis Model, J. Comput. Graph. Stat., 8, 854–888, doi:10.1080/10618600.1999.10474853, 1999.

Paatero, P., and Tapper, U.: Positive matrix factorization: A non-negative factor model with optimal utilization of error estimates of data values, Environmetrics, 5, 111–126, doi:10.1002/env.3170050203, 1994.

Paatero, P., Hopke, P. K., Song, X. H., and Ramadan, Z.: Understanding, and controlling rotations in factor analytic models, Chemom. Intell. Lab. Syst., 60, 253–264, doi:10.1016/S0169-7439(01)00200-3, 2002.

Paatero, P., Hopke, P. K., Begum, B. A., and Biswas, S. K.: A graphical diagnostic method for assessing the rotation in factor analytical models of atmospheric pollution, Atmos. Environ., 39, 193–201, doi:10.1016/j.atmosenv.2004.08.018, 2005.

Polissar, A. V., Hopke, P. K., Paatero, P., Malm, W. C., and Sisler, J. F.: Atmospheric aerosol over Alaska 2. Elemental composition, and sources, J. Geophys. Res. Atmos., 103, 19045–19057, doi:10.1029/98JD01212, 1998.

Sauvage, S., Plaisance, H., Locoge, N., Wroblewski, A., Coddeville, P., and Galloo, J. C.: Long term measurement, and source apportionment of non-methane hydrocarbons in three French rural areas, Atmos. Environ., 43, 2430–2441, doi:10.1016/j.atmosenv.2009.02.001, 2009.

Seibert, P., Kromp-Kolb, H., Baltensperger, U., Jost, D. T., and Schwikowski, M.: Trajectory analysis of high-alpine air pollution data, in Air Pollution Modeling, and Its Application X, edited by S.-E. Gryning, and M. M. Millán, pp. 595–596, Springer, Boston, MA., 1994.